Current Applied Science and Technology Vol. 23 No. 1 (January-February 2023)

Research article

Evaluation of Coating Ability of TiO_2 Nanoparticles onto Aluminum Alloy Sheet by Physicochemical Analysis

Khatcharin Wetchakun[1]* and Natda Wetchakun[2,3]

[1]*Program of Physics, Faculty of Science, Ubon Ratchathani Rajabhat University, Ubon Ratchathani, Thailand*
[2]*Photocatalysts and 2D Materials Research Laboratory, Department of Physics and Materials Science, Faculty of Science, Chiang Mai University, Chiang Mai, Thailand*
[3]*Center of Excellence in Materials Science and Technology, Chiang Mai University, Chiang Mai, Thailand*

Received: 21 January 2022, Revised: 9 May 2022, Accepted: 2 June 2022

DOI: 10.55003/cast.2022.01.23.007

Keywords

aluminum;
chemical sintering;
wet coating;
doctor-blade;
thin film;
titanium dioxide

Abstract

TiO_2 nanoparticle films were successively coated onto aluminum (Al) alloy sheet using a coating technique at 150°C for 5 h. This was a chemical sintering method, integrated with Al/TiO_2/Al sandwich coupling and used weak acid as a binder. To evaluate the coating ability of the TiO_2 nanoparticles on the aluminum alloy sheet, the physicochemical characteristics of the film samples were analyzed by means of SEM-EDS, FT-IR and XRD. The TiO_2 films prepared by the coating technique at 150°C for 5 h were compared with TiO_2 films prepared by the doctor-blade technique at 500°C for 10 min using two different organics as binders. The results of the physicochemical analysis indicated that the coating technique at 150°C for 5 h provided superior coating ability of TiO_2 nanoparticles onto aluminum alloy sheet than the doctor-blade technique. This may have been because of reduction of the thermal gradient at the TiO_2 interface, which affected the relaxation of internal and external stresses on the TiO_2 film on the aluminum alloy substrate. In this work, the TiO_2 film prepared by chemical sintering method, integrated with Al/TiO_2/Al sandwich coupling at 150°C for 5 h using weak acid mixed with 5 wt.% ammonia as a binder proved to produce the optimum TiO_2 film; however, film thickness control using the coating technique at 150°C for 5 h still needs to be developed.

*Corresponding author: Tel.: (+66) 45352000-29 Fax: (+66) 45352070
E-mail: khatcharin.w@ubru.ac.th

1. Introduction

Aluminum alloy has been used in various applications due to its dominant properties such as low-cost [1], light-weight [2], tunable mechanical strength [3] and light reflection [4]. Titanium dioxide (TiO_2) is a potential material for anti-corrosive protection, antimicrobial action and organic degradation under UV light. Up to now, TiO_2 film has been coated on various substrates such as glass, plastic, nickel, titanium, and stainless steel and aluminum [5]. The coating ability of TiO_2 nanoparticles onto aluminum alloy sheet depends on a pretreatment process that induces adhesive bonding between the adhesive and the adherent [6, 7]. High surface energy, surface roughness and surface cleanliness of aluminum alloy affect the achievement of good adhesive bond strength [8]. The pretreatment of aluminum alloy surfaces for adhesive joining can be made through a surface modification with removal of the oxide layer. The surface pretreatment of aluminum alloy can be simply and effectively carried out by alkaline immersion. For example, Saleema *et al*. [9] found that immersing aluminum substrates in a very dilute solution of sodium hydroxide (NaOH) can help produce a rough surface and improve adhesive bonding. On the other hand, etching aluminum alloy surface with acid produces a porous pitted surface on the aluminum alloy [10]. Previous research [8] reported good adhesion between aluminum alloy and epoxy resin as an adhesive by degreasing the aluminum alloy in alkaline solution and subsequently etching it in acid solution. Moreover, Zhou *et al*. [3] found that alkaline cleaning before acidic pickling can improve the corrosion resistance of Zr conversion coating on 6061 aluminum alloy. In previous research, TiO_2 coating onto aluminum was made using wet and dry coating methods such as dip-coating [11-17], atomic layer deposition [4, 18], and magnetron sputtering [19]. Wet coating methods, such as spraying, dipping, spinning, and the doctor-blade and chemical sintering methods, are of interest because these methods can be conducted at low temperature, are suitable for large-area film and are economical. Most of these methods used for adhering TiO_2 nanoparticles onto substrates have been performed with two types of binder: (i) organic materials such as polyethylene and polyvinylchloride and (ii) weak acids such as acetic acid and citric acid [20]. There are a few previous reports focusing on wet coating methods of TiO_2 film preparation at $\leq$ 150°C without using organic binder. For examples, Park *et al*. [21] fabricated dye-sensitized TiO_2 film coated on a conducting glass substrate using a chemical sintering method, and Miyasaka *et al*. [22] and Lee *et al*. [23] made organic binder-free nano-TiO_2 film for use as a layer in a plastic dye-sensitized solar cell by chemical sintering and the doctor-blade method. In addition, Weerasinghe *et al*. [24] reported fabrication of organic binder-free TiO_2 film coated on plastic substrate by ball milling and spin coating methods, and Li *et al*. [25] reported producing TiO_2 film coated on plastic by a chemical sintering method using inorganic nanoglue as a binder agent for fabricating flexible dye-sensitized solar cells [26, 27]. For the purpose of up-scaling, the doctor-blade method has been reported and widely used in various industries in order to coat inorganic nanoparticles on substrates [28]. Coating by the doctor-blade method, most often done using organic binders as the adhering film onto substrates, is normally followed by an annealing process at high temperature for removal of excess organic binder and sintering of film onto the substrates [29, 30]. To the best of our knowledge, this is the first report on TiO_2 coating on aluminum alloy sheet using the doctor-blade and modified chemical sintering techniques.

This work presents the state-of-the-art in TiO_2 coating on aluminum alloy sheet using a coating technique, integrated with Al/TiO_2/Al sandwich coupling at 150°C for 5 h. The investigation was conducted to fabricate organic binder-free TiO_2 films on aluminum alloy substrates using a chemical sintering method at 150°C for 5 h using weak acid as a binder. The evaluation of the coating technique at 150°C for 5 h using acetic acid as a binder and the doctor-blade technique at 500°C for 10 min with natural latex and 1,2 propanediol as organic binders was investigated by

analyzing the physicochemical characteristics of TiO_2 nanoparticles coated on aluminum alloy substrates.

2. Materials and Methods

2.1 Materials

Aeroxide® P25 TiO_2 nanopowders (Aldrich, Germany; ≥99.5% trace metal basis; particle size: 21 nm (TEM); surface area: 35-65 $m^2 g^{-1}$) were used for producing TiO_2 films. Aluminum alloy sheets (grade 1100) purchased from Sinsiam Profession Steel and Part Co., Ltd., Bangkok, Thailand, were used as substrates. In the treating process of the aluminum alloy surface, glacial acetic acid (CH_3COOH) of analytical grade (RCI-Labscan, Thailand) and sodium hydroxide (NaOH) 99% of analytical grade (RCI-Labscan, Thailand) were used. Acetic acid was also used in chemical sintering method. For the chemical sintering process, ammonia solution (NH_4OH) 25% of analytical grade (Loba Chemie, India) was used. Natural latex extracted from *Hevea brasiliensis* and 1,2 propanediol (ACS reagent, ≥99.5%) purchased from Sigma-Aldrich, Germany, were used as the organic binders.

2.2 Surface treatment of aluminum alloy sheets

The process of surface treatment of aluminum alloy sheets is illustrated in Figure 1. First, aluminum alloy substrates with size of 20 mm × 20 mm × 0.5 mm were washed ultrasonically with DI water for 10 min and then rinsed with acetone. Second, the substrates were immersed in 1 M NaOH aqueous solution for 10 min. Third, the substrates were immersed in 12.5 and 50.0 vol.% acetic acid solutions for periods of 3 and 7 min. Finally, the substrates were ultrasonically washed with DI water for 30 min and were dried at room temperature. Each substrate was immersed in 12.5 vol.% acetic acid solution for 3 min, selected for next TiO_2 coating step, and denoted as uncoated Al.

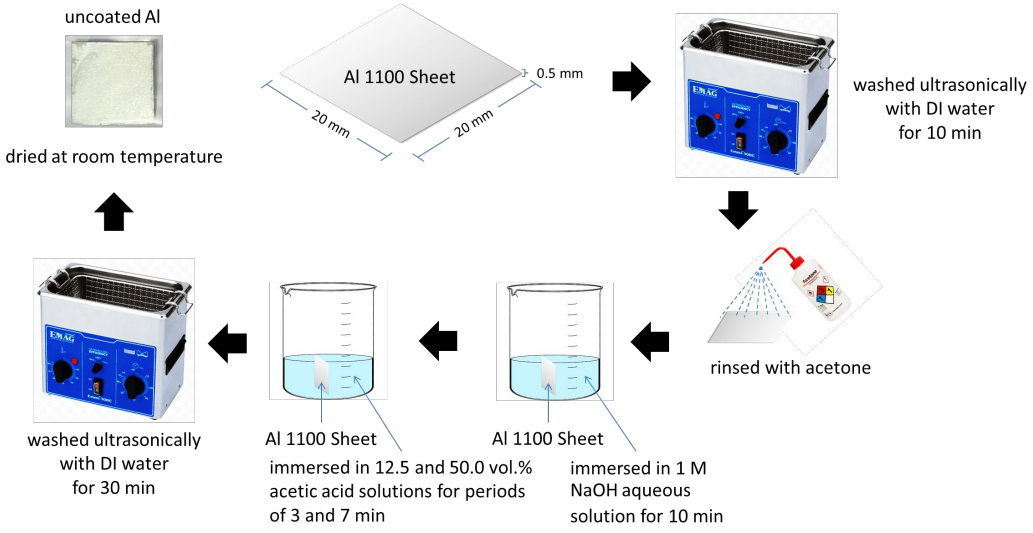

Figure 1. Schematic of surface treatment of aluminum alloy sheets

2.3 TiO_2 coating on aluminum alloy sheets by chemical sintering method (integrated with Al/TiO_2/Al sandwich coupling)

Figure 2 shows the process of TiO_2 coating on aluminum alloy sheets by a chemical sintering method and integrated with Al/TiO_2/Al sandwich coupling, in which the TiO_2 suspension from chemical sintering process (Figure 2(a)) was dropped onto uncoated Al sheet, and then the other sheet was placed on the TiO_2 suspension before heating process (Figure 2(b)). First, 12.5 wt.% TiO_2 suspensions were prepared by mixing 1.313 g TiO_2 nanoparticles with 10 mL of 12.5 vol.% acetic acid solution, and the suspensions were then stirred for 1 h. Second, 10 M ammonia solution was not added or was added into the acidic TiO_2 suspensions to give an acidified 0 wt.% of ammonia (NH_3/TiO_2) concentration, or 5 wt.% of ammonia (NH_3/TiO_2) concentration, and the mixtures were continuously stirred for 72 h. Third, a few drops of each suspension were separately intercalated between two uncoated Al sheets. Therefore, there was a viscous TiO_2 suspension in the middle layer between two uncoated Al sheets. Finally, the TiO_2 nanoparticles on the aluminum alloy sheets were dried at 150°C for 5 h. The prepared TiO_2 films without and with adding 5 wt.% of ammonia (NH_3/TiO_2) concentration were denoted as TiO_2/Al-0(1) and TiO_2/Al-5(1), respectively.

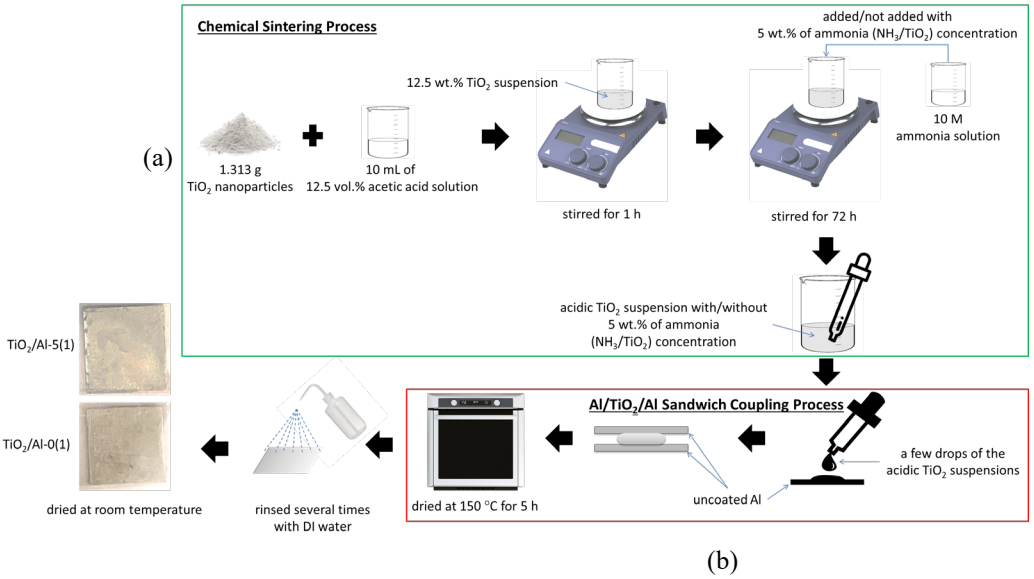

Figure 2. Schematic of TiO_2 coating on aluminum alloy sheets by chemical sintering method integrated with Al/TiO_2/Al sandwich coupling

2.4 TiO_2 coating on aluminum alloy sheets by doctor-blade method

The process of TiO_2 coating on aluminum alloy sheets by the doctor-blade method is presented in Figure 3. First, 1.313 g TiO_2 nanoparticles were ground with 1.6 mL of 1,2 propanediol and 9 vol.% natural latex diluted in distilled water and then cast on uncoated Al sheets. The thickness of TiO_2 films during the doctor-blade coating was controlled by the depth of a blading channel (average 0.15 mm). Second, the TiO_2 nanoparticles on the uncoated Al sheets were dried at room temperature overnight and then dried at 80°C for 6 h. Finally, the TiO_2 nanoparticles on the aluminum alloy sheets were calcined at 500°C for 10 min. The TiO_2 films prepared using 1,2 propanediol and 9 vol.% natural latex as organic binders were denoted as TiO_2/Al-p(2) and TiO_2/Al-n(2), respectively.

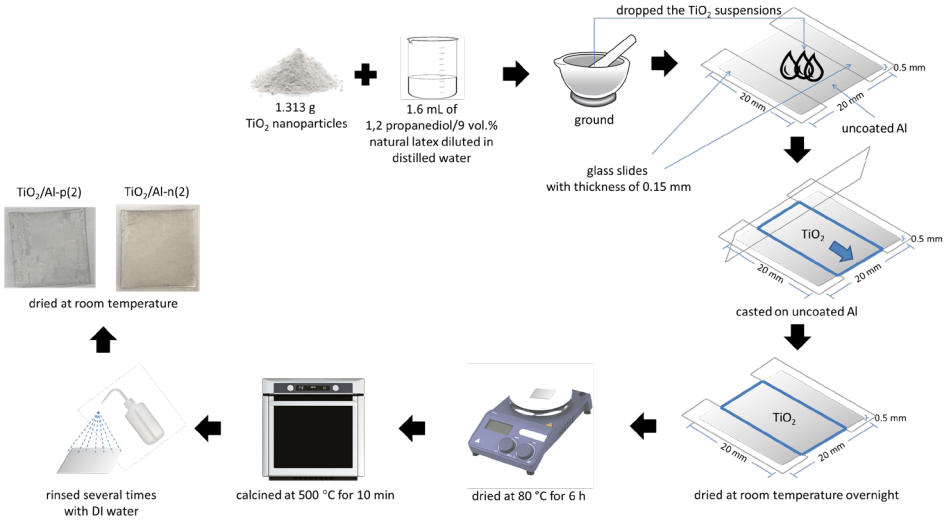

Figure 3. Schematic of TiO_2 coating on aluminum alloy sheets by doctor-blade method

2.5 Physicochemical characterizations

The TiO_2 films coated on uncoated Al sheets were rinsed several times with DI water and then dried at room temperature. The surface morphologies as well as the element compositions of the TiO_2 films were characterized using scanning electron microscope (SEM, JSM-IT300) equipped with an energy dispersive X-ray spectrometry (EDS) system. The thicknesses of the TiO_2 films were measured in the cross-section SEM images of the TiO_2-coated aluminum alloy sheets. To confirm bonding between aluminum alloy sheet and TiO_2 nanoparticles, the TiO_2 films coated on aluminum alloy sheets were analyzed by Fourier transform infrared spectrophotometer (FT-IR, PerkinElmer, Spectrum-RX). TiO_2 film structure was examined by an X-ray diffractometer (SmartLab, Rigaku) using CuKα radiation (λ = 1.5406 Å).

3. Results and Discussion

The untreated aluminum alloy surface (Figure 4a) was smoother than the surface of the aluminum alloy substrate treated by 1 M NaOH for 10 min (Figure 4b). The aluminum alloy substrate immersed in the order of 1 M NaOH solution for 10 min and 12.5 vol.% acetic acid solution for 3 min is shown in Figures 4c-4e. Figure 4c shows that oxide-like layer on the aluminum alloy substrate was slightly peeling at some sites of the substrate. Two different sites were marked with d and e square symbols. Figure 4d presents a magnified image of the site d showing hole sizes of ~1.0-1.5 μm, and Figure 4e presents the magnified image of the site e showing nano-Al_2O_3 aggregate-like morphology. The aggregation of Al_2O_3 nanoparticles corresponds to that seen in a previous report about synthesizing Al_2O_3/Al composites by cementing aluminum containing powders via the hydrothermal method [31]. Under the treatment with 12.5 vol.% acetic acid solution for a prolonged immersion time of 7 min, the surface morphology of the 7 min treated aluminum alloy in Figure 4f was similar to that of the 3 min treated sample in Figure 4c. The peeling of Al_2O_3-like layer on aluminum alloy substrate can be seen after the treatment with 1 M NaOH solution for 10 min and then 50.0 vol.% acetic acid solution for 3 min (Figure 4g). In addition, for the treatment using an

etching time of 7 min with 50.0 vol.% acetic acid solution, an aluminum alloy surface without an Al_2O_3-like layer was observed (Figure 4f).

The scanning electron micrograph of uncoated Al (Figure 5a) shows the smooth surface of the treated aluminum alloy sheet and the small proportion of aluminum fractions. The analysis of the element composition in weight percentage of uncoated Al (Table 1) confirms the presence of aluminum oxide and silicon in agreement with that of Al-1100 alloy as reported by Jamwal *et al*. [32]. As compared with TiO_2/Al-0(1) (Figure 5b), the surface of TiO_2/Al-5(1) (Figure 5c) is flat and does not contain any cracks. This fact indicates that the ammonia addition at 5 wt.% of ammonia (NH_3/TiO_2) concentration in the chemical sintering process decreases the number of cracks and increases partial coalescence. Because it is part of the neutralization process, the addition of aqueous ammonia solution can help increase of electrolyte concentration as shown in equation (1) [6].

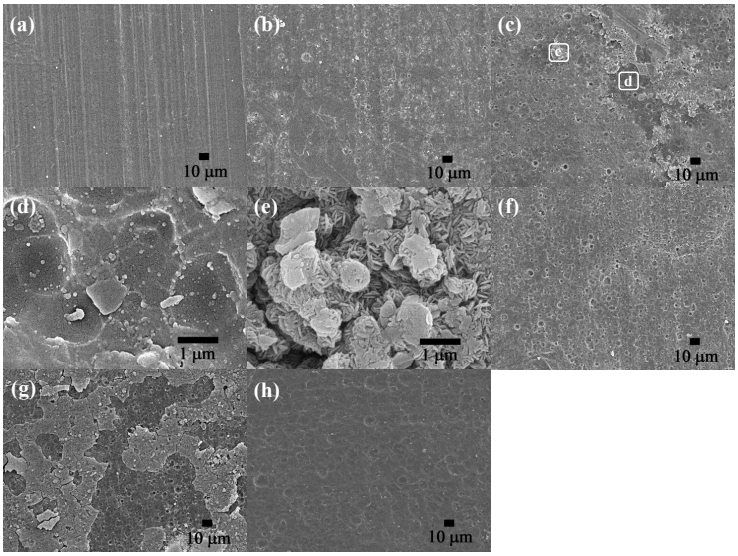

Figure 4. SEM images with 500× magnification of (a) untreated aluminum alloy substrates and aluminum alloy substrates treated with (b) 1 M NaOH solution for 10 min, (c) 1 M NaOH solution for 10 min and then 12.5 vol.% acetic acid solution for 3 min; (d) and (e) treatment condition as same as (c) with 20,000× magnification, (f) 1 M NaOH solution for 10 min and then 12.5 vol.% acetic acid solution for 7 min, (g) 1 M NaOH solution for 10 min and then 50.0 vol.% acetic acid solution for 3 min and (h) 1 M NaOH solution for 10 min and then 50.0 vol.% acetic acid solution for 7 min

$$CH_3COOH\ (aq) + NH_3\ (aq) \rightarrow CH_3COO^-\ (aq) + NH_4^+ \quad (1)$$

The electrolytes act as a glue to induce flocculation and then to increase the viscosity of the suspension. The surface morphologies of TiO_2/Al-p(2) and TiO_2/Al-n(2) are shown in Figures 5d and 5e, respectively, in which coalescence and agglomeration of TiO_2 nanoparticles can be observed due to heat treatment process at high temperature. The existence of TiO_2 nanoparticles dispersed on the substrate can also be seen. The EDS spectra of TiO_2/Al-0(1), TiO_2/Al-5(1), TiO_2/Al-p(2) and TiO_2/Al-n(2) (Table 1) provide Ti concentrations of 30.56, 28.81, 27.23 and 4.17 wt.%, respectively. These indicate that amount of TiO_2 attached onto uncoated Al using the doctor-

blade method was less than that obtained using the chemical sintering method, integrated with Al/TiO_2/Al sandwich coupling. The result confirmed that the presence of aluminum alloy sheets on both surface sides of TiO_2 film can help attach TiO_2 nanoparticles onto the aluminum alloy sheets. This may be because the reduction of the thermal gradient of the TiO_2 interface affects the relaxation of internal and external stresses of the TiO_2 film on the aluminum alloy substrate [33]. Cross-section SEM images (Figures 6a and 6b), EDS line scanning profiles (Figures 6c and 6d) and element composition in weight percentage (Table 2) of the TiO_2/Al-5(1) and TiO_2/Al-p(2) films confirm the structure of the layer of the aluminum substrate and show the thin and inhomogeneous thickness of the films prepared by these techniques. The amount of TiO_2 particles in Figure 6a is greater than that in Figure 6b, whereas the dispersion of the particles in Figure 6a is less than that in Figure 6b.

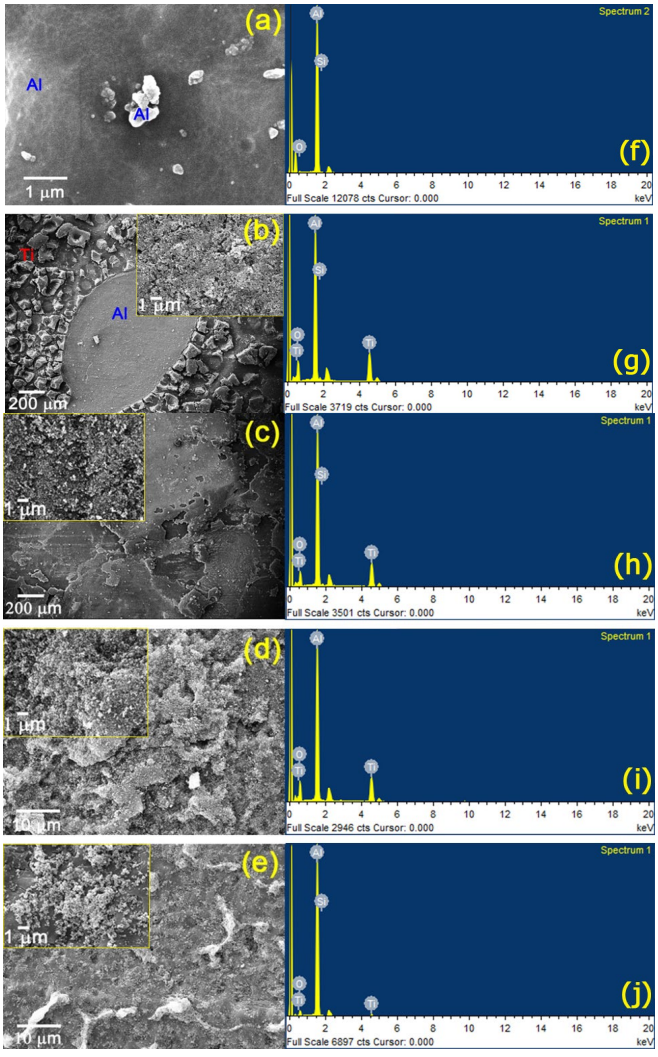

Figure 5. (a), (b), (c), (d) and (e) SEM surface images of uncoated Al, TiO_2/Al-0(1), TiO_2/Al-5(1), TiO_2/Al-p(2) and TiO_2/Al-n(2), respectively; (f), (g), (h), (i) and (j) EDS of total area of (a), (b), (c), (d) and (e), respectively

Table 1. Average elemental composition of uncoated Al, TiO_2/Al-0(1), TiO_2/Al-5(1), TiO_2/Al-p(2) and TiO_2/Al-n(2) from Figure 5 (in wt.%)

Element/Sample	uncoated Al	TiO_2/Al-0(1)	TiO_2/Al-5(1)	TiO_2/Al-p(2)	TiO_2/Al-n(2)
O K	3.69	27.51	21.44	27.25	12.32
Al K	95.81	41.03	49.20	45.52	83.03
Si K	0.50	0.91	0.56	0.00	0.48
Ti K	0.00	30.56	28.81	27.23	4.17

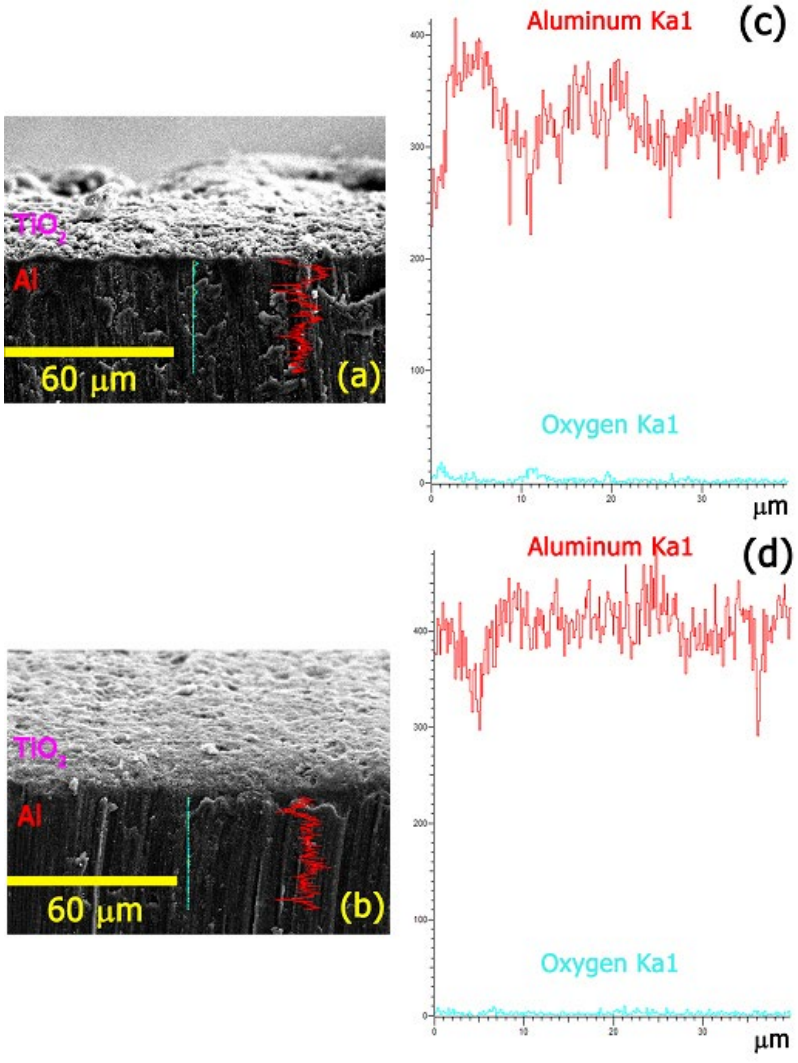

Figure 6. (a) and (b) SEM-EDS cross section images of TiO_2/Al-5(1) and TiO_2/Al-p(2), respectively; (c) and (d) EDS line scanning profiles of (a) and (b), respectively

Table 2. Average elemental composition of TiO_2/Al-5(1) and TiO_2/Al-p(2) from Figure 6 (in wt.%)

Element/Sample	TiO_2/Al-5(1)	TiO_2/Al-p(2)
O K	3.42	2.41
Al K	96.58	97.59

The adhesive coating states of TiO_2 on aluminum alloy sheets in TiO_2/Al-0(1), TiO_2/Al-5(1), TiO_2/Al-p(2) and TiO_2/Al-n(2) specimens were examined by the FT-IR spectra (Figure 7) with the wavenumber in the range of 400-450 cm^{-1}. The band at 660 cm^{-1} of all samples can be attributed to the asymmetric stretching vibration of Al–O [29]. The appearance of overlap between the 400-660 cm^{-1} and 660-870 cm^{-1} bands corresponds to the Ti–O–Ti stretching vibration mode in crystalline TiO_2 [34] and the Al–O stretching mode in crystalline Al_2O_3. This evidence indicates that it is possible that Al and Ti components were connected in the form of Al–O–Ti bond [35]. The presence of crystalline $Al(OH)_3$ can be inferred from the presence of the broad absorption band in the range of 3700-3000 cm^{-1} with reference to –OH group stretching vibration at 1110 cm^{-1} [36] and at 660 cm^{-1}, consistent with the SEM-EDS results. The FT-IR band intensity in the range of 400-450 cm^{-1} of TiO_2/Al-0(1) and TiO_2/Al-5(1) were higher than those of TiO_2/Al-p(2) and TiO_2/Al-n(2). It can be stated that the coating technique at 150°C for 5 h provides higher coating adhesion of TiO_2 film on aluminum alloy sheet than the other technique. This analysis agrees with the SEM-EDS results.

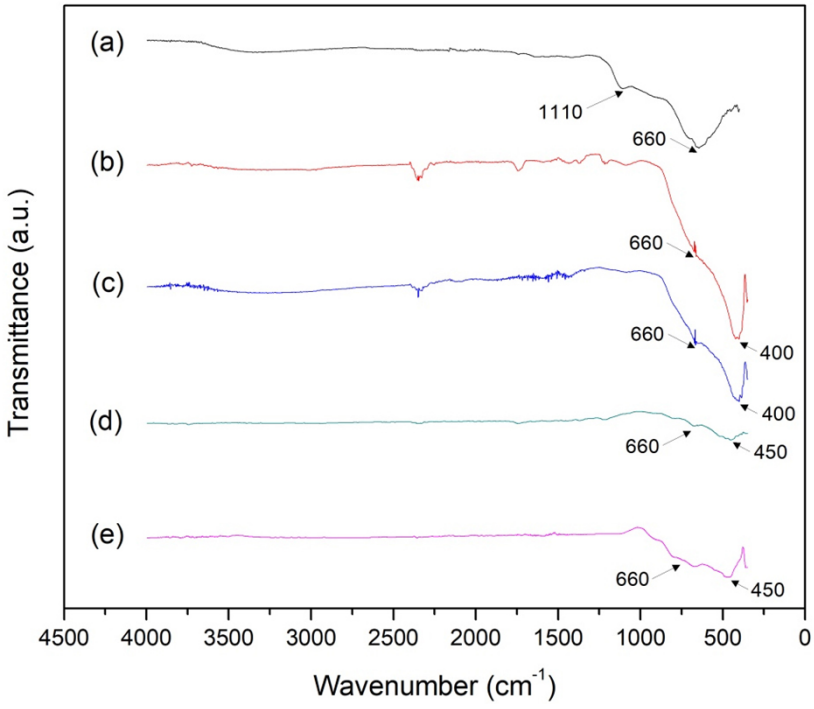

Figure 7. FT-IR spectra of (a) uncoated Al, (b) TiO_2/Al-0(1), (c) TiO_2/Al-5(1), (d) TiO_2/Al-p(2) and (e) TiO_2/Al-n(2)

Uncoated Al showed crystalline aluminum phase according to ICDD reference no. 01-001-1176 and presented as crystalline aluminum trihydroxides of the bayerite and gibbsite phases according to ICDD reference no. 01-074-1119 and 00-007-0324, respectively, as shown in Figure 8. The Bayerite and gibbsite structures of aluminum trihydroxide can result from the immersion of aluminum alloy sheet in strong pH solution with rapid and slow precipitation of aluminum trihydroxide presented as bayerite and gibbsite structures, respectively [37]. The result of XRD peak intensities can indicate that the TiO_2 film prepared using chemical sintering method integrated with $Al/TiO_2/Al$ sandwich coupling has a higher coating adhesion on the aluminum alloy sheet than the TiO_2 film prepared by the doctor-blade method. This is in good agreement with the SEM-EDS and FTIR results. The crystallite sizes (D) of anatase TiO_2 in the A(1 0 1) plane of TiO_2/Al-0(1), TiO_2/Al-5(1), TiO_2/Al-p(2) and TiO_2/Al-n(2) calculated from Scherrer equation: $D = \frac{0.9\lambda}{\beta_{A(101)} \cos\theta}$, where $\beta_{A(101)}$ is the full width at half maximum of the A(1 0 1) reflection, and θ is Bragg's angle of reflection, were 21.79, 22.83, 23.97 and 23.28 nm, respectively. These results can elucidate that the addition of 5 wt.% of ammonia (NH_3/TiO_2) concentration causes the crystallite size to grow bigger through the chemical sintering process. In the case of the doctor-blade method, the crystallite size formed using 9 vol.% natural latex as an organic binder is smaller than that using 1,2 propanediol as an organic binder, which may be due to the effect of viscosities on distinct organic binders.

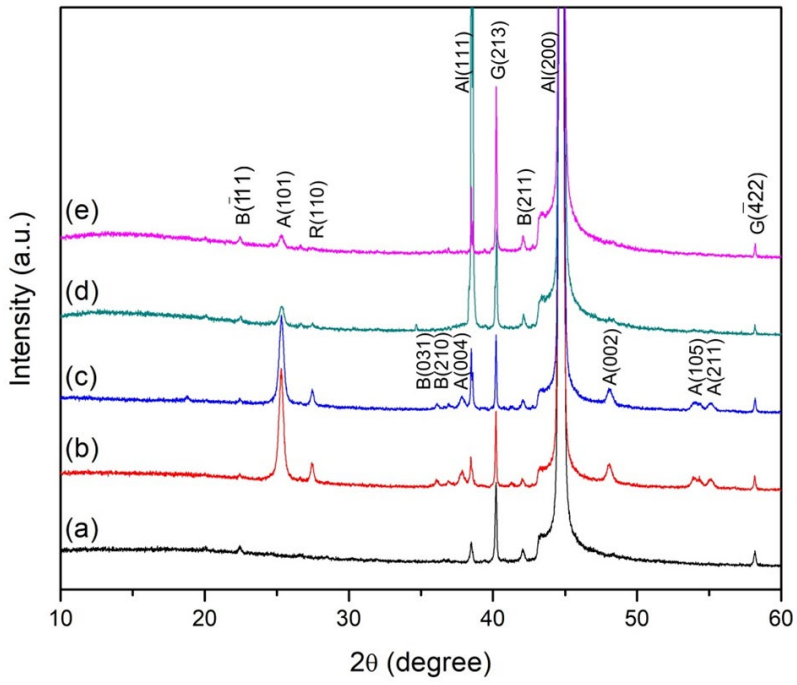

Figure 8. XRD patterns of (a) uncoated Al, (b) TiO_2/Al-0(1), (c) TiO_2/Al-5(1), (d) TiO_2/Al-p(2) and (e) TiO_2/Al-n(2); A, R, B, G and Al symbols on the peaks means anatase, rutile, bayerite, gibbsite and aluminum, respectively.

4. Conclusions

Two coating techniques: (I) chemical sintering method integrated with Al/TiO_2/Al sandwich coupling at 150°C for 5 h using weak acid as a binder and (II) the doctor-blade method at 500°C for 10 min using 1,2 propanediol and 9 vol.% natural latex as organic binders, were evaluated in this work. These two techniques can coat TiO_2 nanoparticles on aluminum alloy sheets. Importantly, the use of technique (I) produces superior adhesive coating of TiO_2 nanoparticles on aluminum alloy sheet than technique (II). The evaluation involved the use of SEM-EDS, FT-IR and XRD. Cross-section SEM images showed that TiO_2 film made from both of coating techniques were of thin thickness; the film from the technique (I) was non-uniform, which was interesting and points to the need for future work concern with improving the wet coating of TiO_2 on aluminum alloy sheet. FT-IR analysis suggested the presence of the Al–O–Ti bond for TiO_2 coated on aluminum alloy substrate. Bayerite and gibbsite crystalline structures appeared in the aluminum alloy substrate after the treatment. The TiO_2/Al-5(1) sample prepared by technique (I) with the addition of 5 wt.% ammonia to the acidic TiO_2 suspension was considered to be the optimum TiO_2 film since it exhibited good adhesion ability as confirmed by SEM-EDS, FT-IR and XRD, and an absence of cracks as confirmed by SEM.

5. Acknowledgements

The authors gratefully acknowledge the support of Ubon Ratchathani Rajabhat University and the Center of Excellence in Materials Science and Technology, Chiang Mai University under the administration of Materials Science Research Center, Faculty of Science, Chiang Mai University. Great appreciation is also extended to Chanthakan Makdi, Fanirat Saithaweep, Porawee Wongsing, Amonrat Hinnak, Pennapa Piwauan and Waraporn Wongcumpuy for assisting the experiment.

References

[1] Li, X.-W., Zhang, Q.-X., Guo, Z., Yu, J.-G., Tang, M.-K. and Huang, X.-J., 2015. Low-cost and large-scale fabrication of a superhydrophobic 5052 aluminum alloy surface with enhanced corrosion resistance. *RSC Advances*, 5(38), 29639-29646.

[2] Pantelakis, S.G. and Alexopoulos, N.D., 2008. Assessment of the ability of conventional and advanced wrought aluminum alloys for mechanical performance in light-weight applications. *Materials and Design*, 29(1), 80-91.

[3] Zhou, P., Liu, Y., Liu, L., Yu, B., Zhang, T. and Wang, F., 2019. Critical role of pretreatment on the corrosion resistance of Zr conversion coating on 6061 aluminum alloy: The combined effect of surface topography and potential difference between different phases. *Surface and Coatings Technology*, 377, DOI: 10.1016/j.surfcoat.2019.124904.

[4] Song, H., Wu, W., Liang, J.-W., Maity, P., Shu, Y., Wang, N.S., Mohammed, O.F., Ooi, B.S., Gan, Q. and Liu, D., 2018. Ultrathin-film titania photocatalyst on nanocavity for CO_2 reduction with boosted catalytic efficiencies. *Global Challenges*, 2(11), DOI: 10.1002/gch2.201800032.

[5] Fu, N., Huang, C., Liu, Y., Li, X., Lu, W., Zhou, L., Peng, F., Liu, Y. and Huang, H., 2015. Organic-free anatase TiO_2 paste for efficient plastic dye-sensitized solar cells and low temperature processed perovskite solar cells. *ACS Applied Materials and Interfaces*, 7(34), 19431-19438.

[6] Arrowsmith, D.J. and Clifford, A.W., 1985. A new pretreatment for the adhesive bonding of aluminium. *International Journal of Adhesion and Adhesives*, 5(1), 40-42.
[7] Withy, B., Hyland, M. and James, B., 2006. Pretreatment effects on the surface chemistry and morphology of aluminium. *International Journal of Modern Physics B*, 20, 3611-3616.
[8] Xu, Y., Li, H., Shen, Y., Liu, S., Wang, W. and Tao, J., 2016. Improvement of adhesion performance between aluminum alloy sheet and epoxy based on anodizing technique. *International Journal of Adhesion and Adhesives*, 70, 74-80.
[9] Saleema, N., Sarkar, D.K., Paynter, R.W., Gallant, D. and Eskandarian, M., 2012. A simple surface treatment and characterization of AA 6061 aluminum alloy surface for adhesive bonding applications. *Applied Surface Science*, 261, 742-748.
[10] Withy, B., Hyland, M. and James, B., 2006. Pretreatment effects on the surface chemistry and morphology of aluminium. *International Journal of Modern Physics B*, 20(25-27), 3611-3616.
[11] Kang, H., Tian, W., Wu, J., Zhang, Y., Li, Z. and Pang, G., 2006. Effect of annealing on microstructure and capacitance properties of sol-gel TiO_2 film on aluminum. *International Journal of Electrochemical Science*, 16(1), DOI: 10.20964/2021.01.21.
[12] Zhao, H., Cao, L., Wan, Y., Yang, S., Gao, J. and Pu, J., 2018. Improving wear resistance of aluminum by hydrophobic sol-gel-derived TiO_2 film. *Industrial Lubrication and Tribology*, 70(8), 1408-1413.
[13] Wang, X., Han, F. and Li, Y., 2014. Effect of aluminum foam support and polyethylene glycol on surface morphology and photocatalytic behavior of TiO_2 films. *Materials Chemistry and Physics*, 145(1-2), 68-74.
[14] Wang, X., Han, F. and Wei, X., 2010. Microstructure and photocatalytic activity of mesoporous TiO_2 film coated on an aluminum foam. *Materials Letters*, 64(18), 1985-1988.
[15] Chen, S.Z., Zhang, P.Y., Zhu, W.P. and Chen, L., 2004. Deactivation of TiO_2 films on titanium, aluminums and glass substrates. *Chinese Journal of Inorganic Chemistry*, 20(11), 1265-1272.
[16] Ikeno, S., Kawabata, T., Hayashi, H., Matsuda, K., Rengakuji, S., Suzuki, T., Hatano, Y. and Tanaka, K., 2002. Fabrication of photocatalytic TiO_2 films on pure aluminum plates. *Materials Transactions*, 43(5), 939-945.
[17] Zhu, Y., Zhang, L., Wang, L., Tan, R. and Cao, L., 2001. Interface diffusion and reaction between TiO_2 film photocatalyst and aluminium alloy substrate. *Surface and Interface Analysis*, 32(1), 218-223, DOI: 10.1002/sia.1041.
[18] Levchuk, I., Guillard, C., Dappozze, F., Parola, S., Leonard, D. and Sillanpää, M., 2016. Photocatalytic activity of TiO_2 films immobilized on aluminum foam by atomic layer deposition technique. *Journal of Photochemistry and Photobiology A: Chemistry*, 328, 16-23.
[19] Daviðsdóttir, S., Dirscherl, K., Canulescu, S., Shabadi, R. and Ambat, R., 2013. Nanoscale surface potential imaging of the photocatalytic TiO_2 films on aluminum. *RSC Advances*, 3(45), 23296-23302.
[20] Gunti, S., Alamro, T., McCrory, M. and Ram, M.K., 2017. The use of conducting polymer to stabilize the nanostructured photocatalyst for water remediation. *Journal of Environmental Chemical Engineering*, 5(6), 5547-5555.
[21] Park, N.-G., Kim, K.M., Kang, M.G., Ryu, K.S., Chang, S.H. and Shin, Y.-J., 2005. Chemical sintering of nanoparticles: a methodology for low-temperature fabrication of dye-sensitized TiO_2 films. *Advanced Materials*, 17(19), 2349-2353.
[22] Miyasaka, T., Ikegami, M. and Kijitori, Y., 2007. Photovoltaic performance of plastic dye-sensitized electrodes prepared by low-temperature binder-free coating of mesoscopic titania. *Journal of The Electrochemical Society*, 154(5), A455-A461, DOI: 10.1149/1.2712140.
[23] Lee, K.-M., Wu, S.-J., Chen, C.-Y., Wu, C.-G., Ikegami, M., Miyoshi, K., Miyasaka, T. and Ho, K.-C., 2009. Efficient and stable plastic dye-sensitized solar cells based on a high light-harvesting ruthenium sensitizer. *Journal of Materials Chemistry*, 19(28), 5009-5015.

[24] Weerasinghe, H., Sirimanne, P.M., Simon, G.P. and Cheng, Y., 2009. Fabrication of efficient solar cells on plastic substrates using binder-free ball milled titania slurries. *Journal of Photochemistry and Photobiology A: Chemistry*, 206(1), 64-70.

[25] Li, Y., Yoo, K., Lee, D.-K., Kim, J.Y., Son, H.J., Kim, J.H., Lee, C.-H., Míguez, H. and Ko, M.J., 2015. Synergistic strategies for the preparation of highly efficient dye-sensitized solar cells on plastic substrates: combination of chemical and physical sintering. *RSC Advances*, 5(94), 76795-76803.

[26] Bresser, D., Mueller, F., Fiedler, M., Krueger, S., Kloepsch, R., Baither, D., Winter, M., Paillard, E. and Passerini, S., 2013. Transition-metal-doped zinc oxide nanoparticles as a new lithium-ion anode material. *Chemistry of Materials*, 25(24), 4977-4985.

[27] Li, Y., Lee, W., Lee, D.-K., Kim, K., Park, N.-G. and Ko, M.J., 2011. Pure anatase TiO_2 "nanoglue": An inorganic binding agent to improve nanoparticle interconnections in the low-temperature sintering of dye-sensitized solar cells. *Applied Physics Letter*, 98(10), DOI: 10.1063/1.3562030.

[28] Yang, H. and Jiang, P., 2010. Large-scale colloidal self-assembly by doctor blade coating. *Langmuir*, 26(16), 13173-13182.

[29] Takahashi, S., Neuville, D.R. and Takebe, H., 2015. Thermal properties, density and structure of percalcic and peraluminus $CaO–Al_2O_3–SiO_2$ glasses. *Journal of Non-Crystalline Solids*, 411, 5-12.

[30] Poh, S., Ahmad, H., Ting, C., Tung, H. and Jun, H., 2021. Performances of flexible dye-sensitized solar cells fabricated with binder-free nanostructure TiO_2. *Journal of Materials Science: Materials in Electronics*, 32(9), 12031-12041.

[31] Haul, R., Gregg, S.J. and Sing, K.S.W. 1982. *Adsorption, Surface Area and Porosity*. London: Academic Press.

[32] Jamwal, A., Vates, U.K., Gupta, P., Aggarwal, A. and Sharma, B.P. 2019. Fabrication and characterization of Al_2O_3–TiC-reinforced aluminum matrix composites. In: K. Shanker, R. Shankar and R. Sindhwani, eds. *Advances in Industrial and Production Engineering . Lecture Notes in Mechanical Engineering*. Singapore: Springer, pp. 349-356.

[33] Kim, J.-I., Kim, J.-K. and Jang, Y.-J., 2019. Stress relaxation through thermal gradient structure of tetrahedral amorphous carbon thin film deposited on Ge–Se–Sb-based chalcogenide glass. *Diamond and Related Materials*, 100, DOI: 10.1016/j.diamond.2019.107547.

[34] Qin, X., Jing, L., Tian, G., Qu, Y. and Feng, Y., 2009. Enhanced photocatalytic activity for degrading Rhodamine B solution of commercial Degussa P25 TiO_2 and its mechanisms. *Journal of Hazardous Materials*, 172(2-3), 1168-1174.

[35] Hu, W., Wan, L., Liu, X., Li, Q. and Wang, Z., 2011. Effect of TiO_2/Al_2O_3 film coated diamond abrasive particles by sol–gel technique. *Applied Surface Science*, 257(13), 5777-5783.

[36] Zawrah, M.F., Defrawy, S.A.E., Ali, O.A.M., Sadek, H.E.H. and Ghanaym, E.E., 2018. Recycling of LCW produced form water plants for synthesizing of nano FeO(OH), $Al(OH)_3$, and layered double hydroxide: Effect of heat-treatment. *Ceramics International*, 44(8), 9950-9957.

[37] Zhang, Y., Chang, J., Zhao, J. and Fang, Y., 2018. Nanostructural characterization of $Al(OH)_3$ formed during the hydration of calcium sulfoaluminate cement. *Journal of the American Ceramic Society*, 101(9), 4262-4274.